# Electro-Thermal Virtual Prototyping of a Rogowski Coil Sensor System

Juan Sebastian Rodriguez Estupiñán, Alain Vachoux
École Polytechnique Fédérale de Lausanne
Microelectronics System Laboratory - LSM
Lausanne, Switzerland CH-1015
Email: juanse.rodriguez@epfl.ch, alain.vachoux@epfl.ch

Joris Pascal
ABB Switzerland Ltd.
Corporate Research
Baden-Dättwil, Switzerland
Email: joris.pascal@ch.abb.com

***Abstract*—An electro-thermal model of a Rogowski Coil sensor system is here described. A co-design methodology between VHDL-AMS and Finite Element Analysis (FEA) has been used for modeling the entire system. The proposed modeling strategy uses geometrical FEA to complete a time-dependent parametrical heat transfer model, which can be implemented in VHDL-AMS or in any other similar hardware description language. This is especially useful for performing simulations with the embedded signal processing electronics of the sensor. Important geometrical, environmental and inner material properties of the Rogowski Coil sensor system, which are difficult, or even impossible to simulate dynamically in a classical lumped-element model, are taken into account indirectly in the proposed model. This allows to study the cross-domain effects in the complete system.**

## I. Introduction

Industrial sensor design is demanding more robust and accurate models which allow to fully predict the effect of cross-domain variables (e.g. temperature, light intensity, pressure, velocity, etc.) into the electrical domain. These variables, which are in many cases difficult to measure and characterize, can influence the system behavior dramatically. Therefore, it is important to include in the analysis of the complete system, dynamic interactions between the variables of other domains and the electrical variables (i.e. analogue or digital). Static cross-domain variables might not describe properly the behavior of the real system.

In this paper we focus on the study of an electrical device for medium-voltage (i.e. tens of kilo volts) applications, based on the Rogowski Coil (RC) transducer. A RC is an electrical instrument for measuring alternating current, which is wrapped around the electrical wire whose current intensity is to be measured, see Fig. 1. It delivers a voltage proportional to the

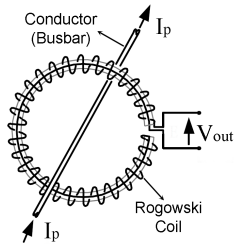


Fig. 1. Rogowski coil sensor and the primary conductor (Busbar) [1].

derivative of the measured current. This type of sensor has many advantages over usual current transformers [2], [3]. It is open-ended, easy to install and much more economic than standard current transformers . The main disadvantage of the RC sensor is its accuracy, which depends on multiple factors such as manufacturing tolerances, the sensor position with respect to the primary current conductor (Busbar), temperature drifts and the degradation of the sensor by aging. In order to improve its accuracy, self-calibration techniques can be applied [4]. Therefore, it is highly desired a trustworthy model (also known as *virtual prototype*) for the complete system design and optimization.

The model must allow to simulate the RC sensor behavior together with its embedded electronics. The ability to deal with both analog and digital signals is very important in the design and test of new RC sensor systems [5]. For this purpose, we have developed a VHDL-AMS electro-thermal model of the RC sensor, see Fig. 2, which is capable of performing transient-parametric simulation of geometrical, thermal and electrical variables. Previous studies for evaluating the RC's sensitivity to the temperature has been reported [6]. Nonetheless, complex systems can include intricate geometries which make difficult, or even impossible, the direct implementation of pure equation-based models. Therefore, Geometrical 3D multiphysics tools based on FEA modeling, are useful to obtain a more accurate model of the complete system.

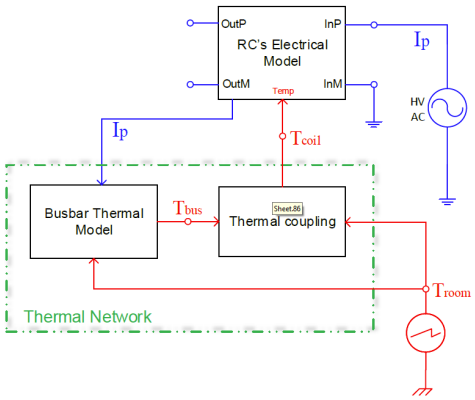


Fig. 2. Block diagram of the Electro-Thermal model of the RC sensor system.

This paper is organized based on the main model components shown in Fig. 2. In Section II, we give our basic assumptions for the thermal modeling of the RC sensor system. Additionally, we introduce the main components of the electro-thermal model. In Section III, we provide a more detailed

978-1-4799-7800-7/15/$31.00 ©2015 IEEE

explanation of the geometrical heat transfer modeling of the RC sensor system. Afterwards, we present an equation-based model extraction of the thermal coupling, which is used for a VHDL-AMS implementation. Finally, simulations of the complete electro-thermal model in VHDL-AMS are given for validation and system analysis.

## II. Model Description

In order to model properly the thermal behavior of the RC sensor system, it is required to adequately describe the heat transfer physics of the coil and its surroundings. For that purpose, we define the following basic assumptions to support the selection of the physics that rule the system behavior:

- The RC sensor system consists of a cylindrical primary conductor (Busbar) and a RC protected by a thick layer of epoxy material that is separated from the Busbar by few millimeters.
- The RC is designed for indoor applications. Therefore, the air velocity around the RC can be ignored.
- The complete RC sensor system is contained in an air box at atmospheric pressure, in which no other heat sources are present.

Changing the previous basic assumptions will lead into changing either, some parameter values (case 1) or, defining a new physics for the system behavior (case 2). The first case is trivial, no major changes to the model are required; for example, the case of inserting a heat source at certain region of the RC sensor system surroundings. The second case is a bit more complex; for instance, the case of inserting an air cooling system will require to use forced convection physics (air velocity different than zero) instead of natural convection.

Taking into account the aforementioned basic assumptions, the electro-thermal model of the RC sensor system can be modeled by 3 parts as is shown in Fig. 2: the RC's electrical model, the thermal model of the Busbar and, the thermal coupling between the Busbar and the RC.

### A. RC's electrical model

The electrical model of the RC sensor is a parametric lumped element model with a distributed architecture based on the work presented in [7] and consistent with the time and frequency experimental responses presented in [8]. This model allows to represent the internal RC impedance in terms of its physical dimensions and the material properties of the coil. Additional parasitic capacitances are also considered. The model supports both transient and frequency-domain simulations.

As it can be observed in Fig. 2, the RC's electrical model has four electrical ports (shown in blue) and one thermal port (shown in red). The electrical input (`InP` and `InM`) of RC is modeled by two electrical terminals connected by a resistor of 1 Ω. In this way, the magnitude of the current through the Busbar ($I_p$) is equal to the applied AC high-voltage. By magnetic induction, $I_p$ causes an AC voltage of the same frequency but only few tens of volts between the electrical output of the RC (`OutP` and `OutM`). Additionaly, $I_p$, which is used to calculate the Joule heating of the Busbar, is injected to the thermal model of the Busbar by using an output quantity port as is shown in the entity declaration of Fig. 3.

In order to make the electrical model of the RC sensor compatible with the heat transfer interactions, the equations of the internal lumped impedances and the coil mutual inductance

```
Library IEEE;
use IEEE.electrical_systems.all;
use IEEE.thermal_systems.all;
...

Entity Rogowski_Coil_Electrical is
...
port ( Terminal InP, InM : electrical;
       Terminal OutP, OutM : electrical;
       Quantity Iin  : out current; -- Busbar current
       Quantity Temp : in temperature );  -- Tcoil [K]
End Entity Rogowski_Coil_Electrical;

Architecture Behavioral of Rogowski_Coil_Electrical is
...
Function Rout(TempK : real) return real is
  begin
  return LW * R_LIN * (1.0 + TCR * (TempK-T0_K));
End Function Rout;
Quantity Rcoil  : resistance; -- Free electrical quantity
Begin
  Rcoil == Rout(Temp);  -- coil resistance (ohm)
...
End Architecture Behavioral;
```

Fig. 3. Fraction of the VHDL-AMS code of the RC's electrical model. `LW` is the wire length in meters, `R_LIN` is the wire resistance per meter, `TCR` is the temperature coefficient of resistance of the wire and `T0_K` is the reference temperature in Kelvin.

are made temperature dependent. Typically, the temperature, like other cross-domain variables, is included in the electrical circuit model as a constant parameter. However, this approach is not convenient for modeling properly the multiphysics interaction between electrical and thermal quantities. We have used VHDL-AMS quantities for both thermal and electrical variables; consequently, the model allows to estimate dynamically the effect of the temperature into the RC internal impedances and the coil mutual inductance.

Let us explain this idea by describing how we have included the RC temperature ($T_{coil}$) and its effect in the RC resistance ($R_{coil}$). We can consider two different approaches for including dynamic effects of the temperature in the electrical model of the RC. The first option consist on using a thermal terminal. The VHDL-AMS terminals guarantee the energy conservation in its related quantities. Therefore, a bidirectional coupling between the electrical and thermal quantities can be simulated. However, we do not need to consider the RC self-heating, since the current inside the RC winding is low enough, in the order of few mA. Hence, we have used a second option, to include the temperature using an input quantity port as is shown in Fig 3. In this way, the temperature of the RC is calculated in the thermal network and simply passed to the RC's electrical model to calculate the aforementioned temperature dependent electrical variables. In Fig. 3 we can observe that $R_{coil}$ is calculated through the function `Rout`, which changes with the temperature given by the quantity port `Temp`. Likewise, the dynamic value of the internal lumped impedances can be transferred via quantity ports; an example is given for a simple resistor architecture in Fig. 4.

### B. Busbar thermal model

The problem of calculating the temperature of a power conductor is explained in detail in the literature, see [9] and [10]. The temperature of the conductor ($T$) can be obtained by the conductor's heat balance differential equation as follows:

$$m_c \cdot C_p \cdot \frac{dT}{dt} = Q_J + Q_M - Q_R - Q_C \qquad (1)$$

where $m_c$ is the conductor's mass per unit length, $C_p$ is the specific heat capacity at constant pressure, $Q_J$ is the Joule

```
Entity Resistor_quantity is
  Port ( Quantity R : in resistance;
         Terminal NP , NN : electrical );
End Entity Resistor_quantity;

Architecture simple of Resistor_quantity is
  Quantity v across i through NP to NN;
Begin
  v == i * R;
End Architecture simple;
```

Fig. 4. VHDL-AMS dynamic resistor model.

heating, $Q_M$ is the heat generated by magnetic losses (i.e. skin and spiral effects), $Q_R$ and $Q_C$ are the energy loss by radiation and convection respectively.

The Busbar thermal model can be specified by means of an equivalent lumped-element circuit analogy or by using directly the differential equations in the model. As VHDL-AMS language allows to directly express the equations in the model, we decided to use the equation-based approach by implementing the Busbar thermal model with the Equation 1 together with the equations of the IEEE Standard 738-2006 [10]. The equivalent lumped-element circuit approach introduces unnecessary circuit bias which might lead to inaccuracies in simulation.

### C. Thermal coupling model

This model represents the thermal coupling between the Busbar and the RC, i.e. the heat transfer from the Busbar surface to the environment passing through the RC geometry. Modeling properly this interaction is the challenge of this work. As is depicted in Fig. 2, the effective temperature of the RC ($T_{coil}$), is calculated in this model from both the Busbar temperature ($T_{bus}$) and the room temperature ($T_{room}$). This problem can be classically simplified by considering the thermal coupling as a thermal circuit with two thermal resistors connected in series, one thermal resistance between the Busbar and the RC, and the other between the RC and the environment. The problem of this simplification lies in the difficulty to calculate accurately the values of the two thermal resistances. In fact, it is not required to calculate each thermal resistance independently, but the ratio between them is the important value. However, this simplification does not help to determine such ratio.

The idea is to obtain a parametric expression for the thermal coupling, i.e. a $T_{coil}$ equation as a function of $T_{bus}$, $T_{room}$ and any other material or geometric parameter of the RC sensor, for instance, the air gap between the Busbar and the RC surface ($A_{gap}$). One of the main problems for obtaining a direct parametric equation for the RC temperature relies on the geometry of the system. The heat transfer equations (steady-state or time-dependent equations) need to be solved for the complete geometry. This is why, we have chosen to model the RC sensor system by a different approach, namely Finite Element Analysis (FEA). The model has been implemented in COMSOL Multiphysics (4.3b), which allows to simulate the heat transfer behavior along the entire RC sensor geometry.

In this work, FEA modeling is used for two purposes: Firstly, to find out a parametric equation-based model of the thermal coupling block. Secondly, to serve as a validation reference for the electro-thermal model of the RC sensor system in VHDL-AMS. This is especially important since accurate measurements of $T_{coil}$ are complicated to obtain in the real system.

## III. Electro-Thermal Modeling

Building a heat transfer FEA model requires several steps. First, define the proper outer boundary of the system. Second, choose the correct physics. Third, build the geometry. Fourth, define and assign materials and other parameters. Fifth, define initial values, domain and internal boundary conditions. And finally, mesh the geometry. In that way, the model is ready for simulation and post-processing. By following these steps, the thermal model of the RC is here explained.

### A. RC's heat transfer model

In order to clearly define the outer boundary of the system we need to consider our thermal model closed at some distance. In general, the description of the system must be chosen in such a way that it resolves the fine structure of the model only to the degree of interest. Therefore, we assume that the RC sensor system is contained in an air box at atmospheric pressure. At this level, there are three fundamental boundary conditions: 1) prescribed temperature (*Dirichlet condition*); 2) prescribed normal flux (*Neumann condition*); and 3) a convective heat flux (*Robin-Cauchy condition*). We have used the third condition as it represents a mix of the two first cases, this is expressed as follows:

$$\mathbf{n} \cdot \mathbf{q} = h\,(T_{ext} - T) \tag{2}$$

where $\mathbf{n} \cdot \mathbf{q}$ is the heat flux normal at the boundary wall, $h$ is the heat transfer coefficient and $T_{ext}$ is the external temperature.

The next step consists on determining the type of heat transfer processes which appear in the RC sensor system. From the previous mentioned modeling assumptions, the dominant heat transfer processes are conduction in solids (in the RC and the Busbar) and free natural convection in the surrounding air. Hence, a complete thermal model of the RC sensor system includes the heat convection-diffusion (Equation 3) without considering viscous heating and pressure work, conservation of mass in a Non-Isothermal flow (Equation 4), and Navier-Stokes for free convection (Equation 5):

$$\rho C_p \frac{\partial T}{\partial t} + \rho C_p \mathbf{u} \cdot \nabla T = \nabla \cdot (k \nabla T) + Q \tag{3}$$

$$\frac{\partial \rho}{\partial t} + \nabla \cdot (\rho \mathbf{u}) = 0 \tag{4}$$

$$\rho \frac{\partial \mathbf{u}}{\partial t} + \rho \mathbf{u} \cdot \nabla \mathbf{u} = \nabla \left[ -p\mathbf{I} + \mu \left( \nabla \mathbf{u} + (\nabla \mathbf{u})^T \right) - \frac{2}{3} \mu (\nabla \mathbf{u}) \mathbf{I} \right] + \Delta \rho(T) g \tag{5}$$

where $\rho$ is the fluid density, $\mathbf{u}$ is the velocity vector, $k$ is the thermal conductivity, $\mu$ is the dynamic viscosity, $p$ is the pressure, $g$ is the gravity force, and $Q$ contains all the heat sources. A Conjugated Heat Transfer (CHT) model solves the system through a bidirectional coupling of the Equation 3 and 5. This model can only be solved as time-dependent model, since there is no steady-state as the air flow is continuously fluctuating around the RC sensor and the Busbar. However, by ignoring the air velocity (i.e. $\mathbf{u} = 0$), the system can be solved by steady-state simulations only using the Equation 3 for modeling the heat transfer in the air. We call this approximation the Simplified Heat Transfer (SHT) model.

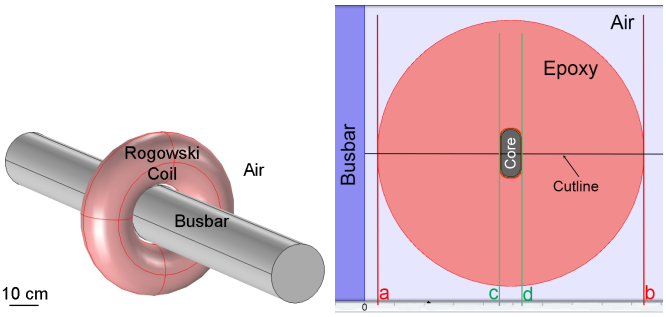


(a) (b)

Fig. 5. (a) 3D geometry of the RC sensor system. (b) 2D axisymmetric geometry (cross-sectional view) of the RC sensor system.

The next step is to create the geometry of the system. In Fig. 5a we can see a 3D view of the RC sensor system. However, the symmetry of the geometry and the heat transfer process (i.e. in a radial direction from the Busbar), allow us to simplify the geometry of the model as is shown in Fig. 5b. Consequently, the number of elements is reduced and the performance of the simulation is improved. By revolving the 2D axisymmetric geometry around its symmetry axis (leftmost vertical line), the 3D geometry is reconstructed.

In a more detailed view of the RC core, we can observe how the RC sensor is wired in Fig. 6a. The RC has a double winding of cooper wire which is insulated by a thin coating of resin. In Fig. 6b we can see how the double winding of cooper in the model is approximated. Instead of recreating geometrically the real winding around the RC core, we have made 2 layers of cooper with a thickness equal to the cooper wire diameter ($d_{wire}$) and we have used the boundary condition 'Thin Thermally Resistive Layer' for modelling the effect of the thin resin coating of the cooper wire. The thickness ($d_{resin} = [d_{sc}/2 - d_{wire}]/2$) and the thermal conductivity ($k_s$) of the insulating resin are used to define the thermal resistance ($R_s = d_{resin}/k_s$) at the boundary.

The internal boundary thickness of the double layer of cooper ($d_{resin\_int}$) is not exactly two times $d_{resin}$, since the second winding of cooper wire is not perfectly aligned with the first winding. Therefore, the $d_{resin\_int}$ is defined as ($F_{fact} \cdot d_{resin}$), where $F_{fact}$ is the filling factor of the double winding. By using this modeling approach is easier to generate a high quality mesh and to avoid typical FEA model problems when trying to mesh a geometry with relatively very small distances.

### B. FEA thermal simulation

In order to simulate the thermal behavior of the RC sensor system without taking into account electrical influences, we assume in this subsection a constant Busbar temperature. In

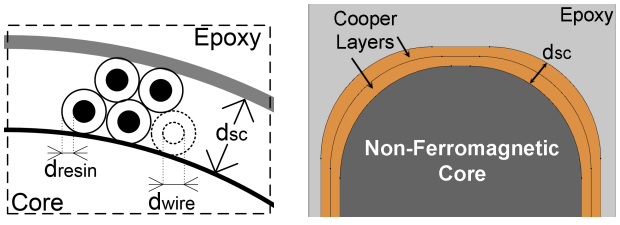


(a) (b)

Fig. 6. (a) Cross-sectional view of the real RC winding (not scaled). (b) 2D axisymmetric RC model geometry. Zoom of the Figure 5b.

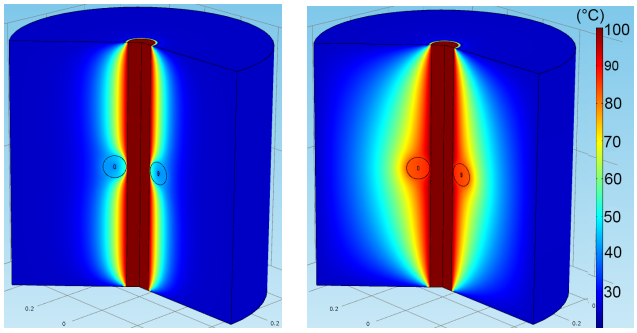


(a) (b)

Fig. 7. 3D revolution temperature plots of the CHT model. $T_{bus} = 100°C$, $T_{room} = 25°C$, $A_{gap} = 4.2mm$. (a) 10 minutes. (b) 3 hours.

fact, we are interested to observe the transient heat transfer behavior and the final steady-state temperature of the RC sensor at operational temperature of the Busbar. Fig. 7. shows two 3D temperature plots at different times in a transient simulation. We can see the evolution of the temperature gradient around the Busbar and the RC. From an initial $T_{room} = T_{ext} = 25°C$, the RC prevents a uniform temperature increasing in the surrounding air at the Busbar, see Fig. 7a. After 3 hours, Fig. 7b, the temperature gradient is practically in steady-state. Although the temperature gradient takes a little longer than 3 hours to be stable, the air flow around the Busbar is always fluctuating due to the energy transfer by natural convection, similar to a boiling water system.

As the temperature gradient reaches the stability, we are motivated to simplify the model by ignoring the air velocity field, i.e. by using the SHT model. In Fig. 8 we can observe a transient simulation of both the CHT and SHT models. At steady-state, the difference between the temperature predictions of the two models is in the order of tens of mili-Celsius as it can be observed in Fig. 8b. Since there is no energy lost by the air movement in the SHT model, $T_{coil}$ is a little higher, the temperature response is a bit faster and slightly under-damped than the CHT model. However, the temperature settling time in both models is about the same.

In order to explain how and where $T_{coil}$ is defined, let us consider Fig. 9. This is a steady-state simulation of the SHT model in which is plotted the temperature throughout a cutline from the Busbar surface (distance = 0 m) to the extreme of the air box. The cutline is taken at the RC geometrical center as is shown in Fig. 5b. The distances a, b, c and d in Fig. 9 correspond to the highlighted distances in Fig. 5b. It can be observed that the temperature decrement is significantly faster in the air region than inside the RC, i.e. the region between a and b. In a closer look in Fig. 9b, we can see that the temperature remains practically constant throughout the RC

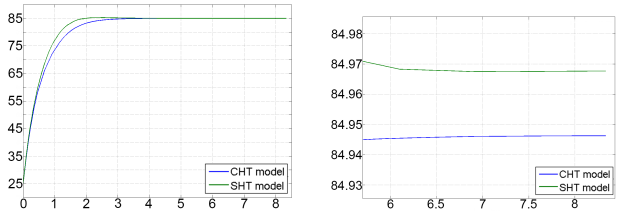


(a) Overall view (b) Zoom

Fig. 8. $T_{coil}$ (°C) vs. Time (hours), CHT and SHT transient simulation. $T_{bus} = 100°C$, $T_{room} = 25°C$, $A_{gap} = 4.2mm$.

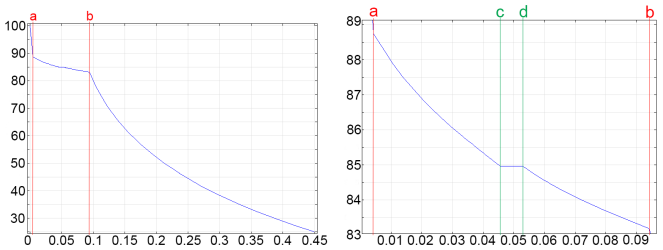


(a) (b)

Fig. 9. Temperature ($^{\circ}C$) vs. Distance (m). SHT static simulation throughout the cutline shown in Fig. 5b. (a) Entire region. (b) Zoom in the RC region.

core, i.e. the region between c and d. Actually, the temperature inside the RC core also decreases with the distance to the Busbar surface. However, the temperature difference between the inner and the outer extreme of the RC core is less than few tens of mili-Celsius. Therefore, we can safely define $T_{coil}$ as the temperature at any point inside c and d.

### C. Equation-based model of the thermal coupling

From the transient behavior of the CHT/SHT model, we can estimate the transient behavior of $T_{coil}$ using the following Equation:

$$T_{coil}(t) = T_0 + (T_{SS} - T_0)\left(1 - e^{-\frac{t}{\tau}}\right) \tag{6}$$

where $T_0$ is the effective initial temperature of the RC, $T_{SS}$ is the final steady-state temperature of the RC, and $\tau$ is the time constant of the RC sensor. The SHT model can be used for static parametric simulations to obtain $T_{SS}$ at different conditions. Afterwards, a polynomial curve fitting algorithm is performed to obtain the following equation:

$$T_{SS}(T_{bus}, T_{room}, A_{gap}) = \quad P_0 + P_1 T_{bus} + P_2 T_{room} + P_3 A_{gap} \tag{7}$$

where $P_i$ are fitting coefficients which depends on the RC core used.

Likewise, an equation for $\tau$ can also be acquired by polynomial curve fitting. However, $\tau$ can only be obtained by transient simulations. Consequently, its estimation by parametric simulation is highly time consuming and impractical. A good approximation for the time behavior of the thermal coupling model can be made by considering an average (*avg*) or a worst case scenario, i.e. to simulate the maximum (*max*) and minimum (*min*) $\tau$ of the system within the sweep parameter range shown in TABLE 1. After a series of simulations, it has been observed that $\tau$ is highly dependent on $A_{gap}$, and slightly dependent on $T_{bus}$ and $T_{room}$; therefore, $\tau$ is approximated as follows:

$$\tau_x(A_{gap}) = S_3 A_{gap}^3 + S_2 A_{gap}^2 + S_1 A_{gap} + S_0 \tag{8}$$

where $S_i$ are fitting coefficients which depends on the RC core used and the considered case (i.e. $x$ = *min / avg / max*).

| Name | Min | Max | Step |
|---|---|---|---|
| $T_{bus}$ | -5 $^{\circ}C$ | 200 $^{\circ}C$ | 5 $^{\circ}C$ |
| $T_{room}$ | -10 $^{\circ}C$ | 90 $^{\circ}C$ | 5 $^{\circ}C$ |
| $A_{gap}$ | 0 mm | 5 mm | 0.2 mm |

TABLE 1. SWEEP PARAMETER RANGE.

### D. Electro-Thermal Model Simulation and Analysis

By parametric static and transient simulations of the geometrical SHT model, we can get an equation-based model of the thermal coupling by using equations 2, 3 and 4. Afterwards, the model of the Electro-Thermal RC sensor system (ETRCS) shown in Fig. 2 can be completed in VHDL-AMS. It is worth mentioning that this model only fits a particular selection of RC dimensions and materials.

The first step consists to simulate the ETRCS model using the same conditions as the SHT model, see Fig. 10a. We can observe a similar response in terms of settling time and final temperature as in Fig. 8. This validation can also be done for different parameters in the range given in TABLE 1.

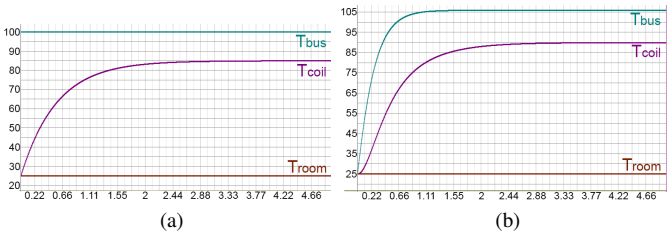


(a) (b)

Fig. 10. Temperature ($^{\circ}C$) vs. Time (hours), ETRCS transient simulations. $A_{gap}$ = 4.2 mm, $T_{room}$ = 25 $^{\circ}C$, $\tau_{avg}$ = 34.14 min. (a) At Constant $T_{bus}$. (b) Using the Standard Busbar model: Input current of 2 $kA_{peak}$ @ 50 Hz.

In a second step, we have simulated the ETRCS model using the IEEE Standard model of the Busbar [10], see Fig. 10b. In this simulation we assume the same initial temperature for the complete system (25 $^{\circ}C$). We can observe how the Busbar increases its temperature thanks to an AC input current; likewise, the RC sensor follows this temperature increment with a lower speed than the Busbar. This can be intuitively understood as the heat transfer goes from the Busbar to the RC sensor.

Finally, we are interested to simulate critical $T_{room}$ variations in the RC sensor system. Fig. 11 shows how the key thermal and electrical variables of the system react to a strong $T_{room}$ fluctuation, an exponential heating up and cooling down between 25 and 80 $^{\circ}C$. The initial condition for this simulation is the operational steady-state temperature of the RC sensor system shown in Fig. 10b. This is a very fast but feasible temperature profile. The heating up process takes more than 30 minutes to achieve the maximum temperature. The cooling down process takes less than 50 minutes to come back to the initial temperature since the falling time constant ($\gamma_f$) is half of the rising time constant ($\gamma_r$). We can see how $T_{bus}$ and $T_{coil}$ are affected by the $T_{room}$ fluctuation, the thermal inertia of the Busbar and the RC are clearly evident from the different marginal changes in their temperature profile with respect to $T_{room}$. We observe slower temperature changes in both the Busbar and the RC, and a small delay for the maximum $T_{bus}$ compared to the maximum $T_{room}$, i.e. around 41.66 minutes.

Fig. 11 also shows the effect of the $T_{room}$ fluctuation in the RC resistance ($R_{coil}$) and the RC inductance ($L_{coil}$). In Fig. 3 and 4 on Section II-A, we have explained how is modeled the temperature effect on $R_{coil}$. Similarly, the temperature dependence of $L_{coil}$ is modeled from the same idea but using a different temperature coefficient. Consequently, both electrical variables have the same wave form as $T_{coil}$.

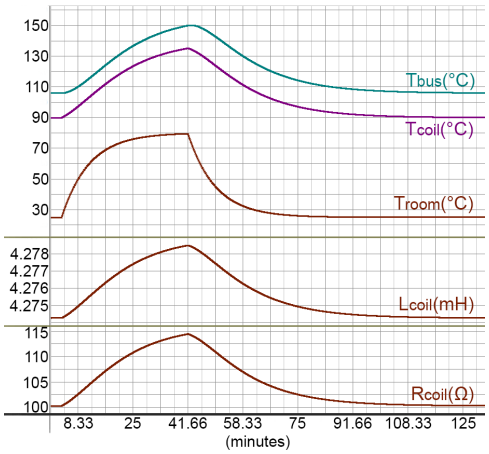


Fig. 11. ETRCS transient simulation. Vertical axes: Temperature (upper graph), Inductance (middle graph), Resistance (bottom graph). Exponential time constants for $T_{room}$: $\gamma_r = 500$ sec (rising), $\gamma_f = 1000$ sec (falling). Initial temperature condition: $T_{bus} = 105.9°C$, $T_{coil} = 88.9°C$ and $T_{room} = 25°C$.

In order to quantify the effect of the $T_{room}$ variation on the electrical variables, we can define the relative variable change as follows:

$$\Delta M = \frac{(M_{max} - M_{min})}{M_{min}} * 100 \tag{9}$$

where $M$ is the specific electrical variable. In Fig. 11, the relative $R_{coil}$ change ($\Delta R_{coil}$) is about 14%, whereas the relative $L_{coil}$ change ($\Delta L_{coil}$) is only about 0.0992%. This significative difference is mainly due to we have used in simulation a temperature coefficient of inductance (TCL) two orders of magnitude lower than the temperature coefficient of resistance of cooper (TCR = 0.0039 $K^{-1}$).

This type of simulation can be used to test the system under different room temperature conditions. Although the ETRCS model can give results for divergent $T_{room}$ profiles, it is important to consider realistic fluctuations in terms of variation speed and wave form. This is especially important to validate this model by using experimental measurements. Moreover, non-commercial RC applications, in which very low temperatures might appear in the system (such as in [11]), could benefit from this co-design methodology between VHDL-AMS and FEA. However, it is important to know the validity range of the thermal and electrical models. Further modifications to the physics and other assumptions in the model can be done for studies under extreme temperature conditions.

## IV. Conclusion

We exploit the multi-domain capabilities of VHDL-AMS together with geometrical FEA to create a versatile parametric model, which can be used for both thermal and electrical simulations. We further improve a classical lumped-element electrical model of the Rogowski Coil to support the dynamic effect of temperature. We show that the proposed electro-thermal model can estimate dynamically the internal temperature of the coil and its dependency on geometrical, electrical and thermal parameters of the system. Furthermore, the model is able to simulate critical temperature fluctuations in the system caused by room temperature drifts. This is very important for a better understanding of the temperature effects in the electrical variables of the sensor and the direct implication in its signal processing electronics. Both electrical and thermal measurements are required for a complete validation of the model here proposed.

## References

[1] W. Ray and C. Hewson, "High performance rogowski current transducers," in *Conference Record of the 2000 IEEE Industry Applications Conference, 2000*, vol. 5, 2000, pp. 3083–3090 vol.5.

[2] M. Samimi, A. Mahari, M. Farahnakian, and H. Mohseni, "The rogowski coil principles and applications: A review," *IEEE Sensors Journal*, vol. 15, no. 2, pp. 651–658, Feb. 2015.

[3] A. Marinescu, "A calibration laboratory for rogowski coil used in energy systems and power electronics," in *2010 12th International Conference on Optimization of Electrical and Electronic Equipment (OPTIM)*, May 2010, pp. 913–919.

[4] G. Meijer, M. Pertijs, and K. Makinwa, *Smart Sensor Systems: Emerging Technologies and Applications*. Delft University of Technology, the Netherlands: John Wiley and Sons, May 2014.

[5] M. Zhang, K. Li, S. He, and J. Wang, "Design and test of a new high-current electronic current transformer with a rogowski coil," *Metrology and Measurement Systems*, vol. 21, no. 1, pp. 121–132, 2014. [Online]. Available: http://www.degruyter.com/view/j/mms.2014.21.issue-1/mms-2014-0012/mms-2014-0012.xml

[6] H. Wang, F. Liu, H. Zhang, and S. Zheng, "Analysis of the thermal expansion effect on measurement precision of rogowski coils," in *International Conference on Power Electronics and Drives Systems, 2005. PEDS 2005*, vol. 2, 2005, pp. 1658–1661.

[7] V. Dubickas and H. Edin, "High-frequency model of the rogowski coil with a small number of turns," *IEEE Transactions on Instrumentation and Measurement*, vol. 56, no. 6, pp. 2284–2288, 2007.

[8] E. Hemmati and S. Shahrtash, "Investigation on rogowski coil performance for structuring its design methodology," *IET Science, Measurement Technology*, vol. 7, no. 6, pp. 306–314, Nov. 2013.

[9] P. Nefzger, U. Kaintzyk, and J. F. Nolasco, *Overhead Power Lines: Planning, Design, Construction*. Springer, Apr. 2003.

[10] IEEE Power Engineering Society, "IEEE standard for calculating the current-temperature of bare overhead conductors," IEEE-SA Standards Board, Standard IEEE Std 738-2006, Nov. 2006.

[11] P. Moreau, A. Le-Luyer, P. Malard, P. Pastor, F. Saint-Laurent, P. Spuig, J. Lister, M. Toussaint, P. Marmillod, D. Testa, S. Peruzzo, J. Knaster, G. Vayakis, S. Hughes, and K. M. Patel, "Prototyping and testing of the continuous external rogowski ITER magnetic sensor," *Fusion Engineering and Design*, vol. 88, no. 6–8, pp. 1165–1169, Oct. 2013. [Online]. Available: http://www.sciencedirect.com/science/article/pii/S0920379612005777